Intensive training in adults refines A1 representations degraded in an early postnatal critical period

Xiaoming Zhou*† and Michael M. Merzenich*‡

*The W. M. Keck Center for Integrative Neuroscience, The Coleman Laboratory, and Department of Otolaryngology, University of California, San Francisco, CA 94143; and †College of Life Sciences, East China Normal University, Shanghai 200062, China

The spectral, temporal, and intensive selectivity of neurons in the adult primary auditory cortex (A1) is easily degraded in early postnatal life by raising rat pups in the presence of pulsed noise. The nonselective frequency tuning recorded in these rats substantially endures into adulthood. Here we demonstrate that perceptual training applied in these developmentally degraded postcritical-period rats results in the recovery of normal representational fidelity. By using a modified go/no-go training strategy, structured noise-reared rats were trained to identify target auditory stimuli of specific frequency from a set of distractors varying in frequency. Target stimuli changed daily on a random schedule. Consistent with earlier findings, structured noise exposure within the critical period resulted in disrupted tonotopicity within A1 and in degraded frequency-response selectivity for A1 neurons. Tonotopicity and frequency-response selectivity were normalized by perceptual training. Changes induced by training endured without loss for at least 2 months after training cessation. The results further demonstrate the potential utility of perceptual learning as a strategy for normalizing deteriorated auditory representations in older (postcritical-period) children and adults.

adult plasticity | cortical plasticity | perceptual training | primary auditory cortex | tonotopic organization

The mammalian auditory system normally undergoes rapid functional maturation after birth. This functional development is substantially influenced by the structure of environmental acoustic inputs in early life, especially within a critical-period time window when the system is most susceptible to alteration by environmental auditory inputs (1–13). Introduction of synchronous inputs into the auditory pathway achieved by exposing rat pups to pulsed noise during this time window, for example, results in a disrupted tonotopicity and broader-than-normal frequency tuning curves in the primary auditory cortex (A1). These changes are not reversed by normal auditory exposure during adulthood, but rather endure throughout life (13).

Earlier studies have shown that sound exposure-induced plasticity recorded in the critical period evolves to support behavioral context-dependent plasticity. When acoustic stimuli are important (closely attended, leading to positive or negative outcomes) to animals of any age, they can generate large-scale remodeling in cortical field A1 (14–23). These earlier studies demonstrated that perceptual learning significantly elaborates temporal, spectral, intensive, and combinative processing selectivity, response strengths, and representational topographies in the adult cortex (14, 15, 19–21). This result contrasts strongly with critical-period plasticity driven by passive exposure to acoustic stimuli; after the closure of the critical period, exposure to the same stimuli has no measurable impact on cortical auditory selectivity if those stimuli are behaviorally meaningless (12, 13, 19, 21, 24–27).

The enduring degradation of A1 representations induced by early exposure to modulated noise presumably impairs the cortical processing of behaviorally important acoustic inputs. For human populations, we have hypothesized that language development deficits commonly arise from similarly noisy sound processing (28–31). Deficits in auditory processing manifested in memory-based frequency discrimination tasks arise in infants and children

destined to develop language impairments (32–34). At older ages, such perceptual deficits strongly predict language and reading impairments (35–39). For example, it has been argued that the phonological and language difficulties of children with specific language impairments might arise from a more basic deficit in the spectral processing and recognition of rapidly changing acoustic events (38, 39). Conversely, the performance of specific language impairment children has been shown to be impaired in specific simple memory-based auditory discrimination tasks mainly involving spectral discriminations (35). Again, the largest deficits were recorded when the impaired subject was speed-challenged. The possibly causal relationship between acoustic processing and language abilities is further supported by studies of Merzenich *et al.* (40) and Tallal *et al.* (41), which have shown that speech and language comprehension abilities of specific language impairment children are significantly improved by adaptive computer training aimed at reducing acoustic temporal integration threshold and improving spectral discrimination among these abilities. It has been proposed that the resultant, well refined representation of spectral and temporal details of acoustic features resulting from such training facilitates the encoding of phonemic inputs and syntax, thereby improving speech- and language-processing abilities (35, 40–42).

By using a modified go/no-go task strategy, in this study we trained developmentally impaired [noise-reared (NR)] rats to identify a target auditory stimulus of a specific frequency presented with a set of distractor auditory stimuli to receive food rewards. Tonal receptive fields and the tonotopicity of A1 were then electrophysiologically documented and compared with those of naive controls (CON), as well as those of same-age NR controls and passively stimulated NR (PNR) rats that received sound stimuli identical to those applied to trained rats (but were given free access to food). Perceptual training resulted in the normalization of developmentally degraded frequency representations in these young adults. These studies further demonstrate the potential utility of perceptual learning applied in older children and adults as a strategy for normalizing auditory and language representations.

Results

Experimental (EXP) NR rats (*n* = 5) were trained to identify a target auditory stimulus of a specific frequency from a set of distractor sound stimuli. The target frequency was set randomly at the beginning of each day's training session. As shown in Fig. 1*A Left*, rats continuously nose-poked in each trial to receive food rewards in the early days of training, resulting in a high rate for both target (red line) and nontarget (green line) responses. This strategy
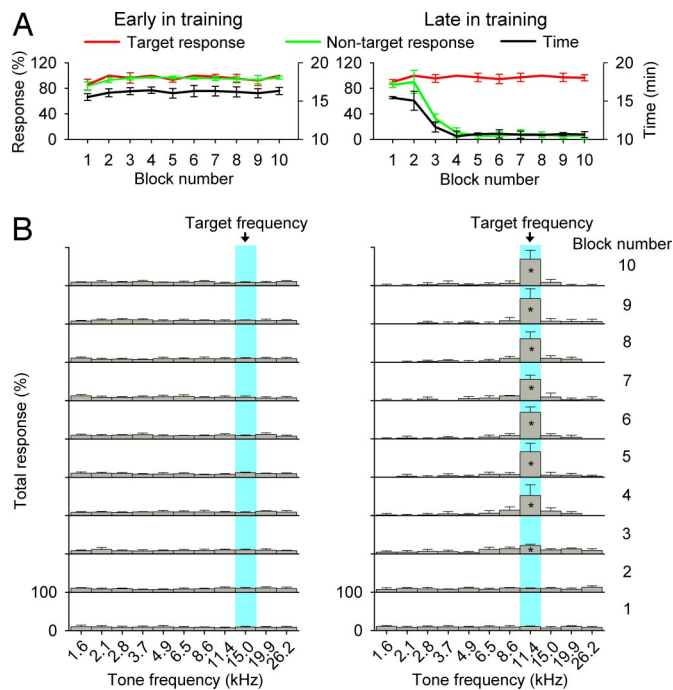
Fig. 1. Behavioral performance on the frequency identification task. (*A*) Target and nontarget responses for each block in the early (*Left*) and the late (*Right*) training day. The time required for rats to complete each block also is shown (right ordinate). (*B*) Distribution of total responses for each block in the early (*Left*) and the late (*Right*) training day. All values shown are mean ± SD. *, $P < 0.01$ ($n = 5$).

resulted in frequent 5-sec time-out periods, during which the house light was turned off and no stimuli were presented. It initially took a long time for rats to finish a training block (average of ≈16 minutes per block; black line in Fig. 1*A Left*). Although there was a modestly lower rate of target and nontarget responses recorded for the first block (which is probably due to acclimatization; repeated-measures ANOVA; $P < 0.01$ for each comparison), there were no significant differences in the rate of target and nontarget responses for the remaining blocks (repeated-measures ANOVA; $P > 0.05$ for each comparison) or in the time used to complete each block (ANOVA; $P > 0.4$) for this early training day. Further analysis showed that nose pokes in each block were equally distributed over all training stimulus frequencies, with no specific clustering on the target frequency (Fig. 1*B Left*; ANOVA; $P > 0.06$ for different blocks).

After several weeks of frequency identification training, rats learned to identify and selectively respond to a new randomly set target frequency on each day. A typical record for a later daily session in trained rats is shown in Fig. 1*A Right*. Note that rats who had mastered the behavior still continuously nose-poked during the initial few blocks, resulting in high rates of both target and nontarget responses (first two blocks in Fig. 1*A Right*). Nose pokes in these blocks were equally distributed over all frequencies of delivered acoustic stimuli, as occurred in the early training epoch (first two blocks in Fig. 1*B Right*; ANOVA; $P > 0.3$ for the first block and $P > 0.09$ for the second block). Starting from the third block, however, nontarget response decreased (green line in Fig. 1*A Right*; repeated-measures ANOVA; $P < 0.001$ for each comparison), whereas the target response still remained at a high rate (red line in Fig. 1*A Right*; ANOVA; $P > 0.09$). These nose pokes for each block sharply favored the target frequency (the third to 10th blocks in Fig. 1*B Right*; repeated-measures ANOVA; $P < 0.01$ for all comparisons of each block). The times used to finish the single training block also significantly decreased from an average of ≈16 min to ≈10 min

(black line in Fig. 1*A Right*; repeated-measures ANOVA; $P < 0.001$ for each comparison).

Immediately after training cessation at approximately postnatal day 90 (P90), neural responses in A1 of the EXP rats were documented by using conventional extracellular unit recording (see *Materials and Methods*). Selectivity of neural responses and cortical maps were then compared with those obtained from the following age-matched animal groups: (*i*) CON ($n = 4$), (*ii*) NR ($n = 5$), and (*iii*) PNR ($n = 5$). High-density maps of A1 were reconstructed from 60- to 100-unit or multiunit recording sites for each animal. The structure (V-shaped, flat-peaked, or multipeaked), selectivity [bandwidth measured at 20 dB above threshold (BW20)], and characteristic frequency (CF) of tuning curves determined at each site, as well as the orderliness of map tonotopicity (tonotopic index), were measured as potential outcomes of perceptual training.

In naive animals, almost all sampled turning curves (97%) were V-shaped with a single CF (Fig. 2*A*, top graph). Most (73%) of these turning curves were relatively sharply tuned to tonal frequencies with BW20s <1.5 octaves. By contrast, only half (50%) of the tuning curves in NR rats were V-shaped. The remainder were either flat-peaked (45%) or multipeaked (5%) (Fig. 2*A*, upper middle graph). Tuning curves with flat peaks across a wide tonal frequency range or with two peaks at different frequencies were typically much more broadly tuned than V-shaped curves. Predominant numbers of these less-selective receptive fields in the A1 of NR rats manifested a degraded spectral selectivity induced by pulsed noise exposure, as shown by Zhang *et al.* (13). The shapes of sampled turning curves from EXP rats, however, were substantially normalized (i.e., all were V-shaped and relatively sharply tuned) (Fig. 2*A*, lower middle graph). No flat- or multipeaked curves (both of which were prominent features of NR rats) were recorded in this group. The sampled tuning curves for PNR rats were comparable to those of NR rats: 54% were V-shaped, 38% were flat-peaked, and 8% were multipeaked (Fig. 2*A*, bottom graph). The distribution of different turning curve types for all recordings obtained in each group is summarized in Fig. 2*B*.

We compared the average BW20s of all tuning curves sampled from different groups of rats (Fig. 2*C*). Here the BW20s were grouped by binning their CF values into five 1-octave-wide categories. As shown in Fig. 2*C*, the average BW20 of NR rats in each CF range ranged between ≈1.5–2.4 octaves, which was significantly larger than that of CON rats (Fig. 2*C*, yellow vs. black bars; repeated-measures ANOVA; $P < 0.001$ for comparison at each CF category). By contrast, after training, the average BW20 decreased to ≈0.9–1.2 octaves in each CF range, significantly smaller than that of NR or PNR rats (Fig. 2*C*, blue bars vs. yellow or pink bars; repeated-measures ANOVA; $P < 0.001$ for both comparisons at each CF category). These values also were smaller than in CON rats, although differences did not quite reach statistical significance (Fig. 2*C*, blue bars vs. black bars; repeated-measures ANOVA; $P > 0.05$ for comparison at each CF category). There also were significant differences in BW20s between NR and PNR rats for CF categories centered at 1.5 and 3 kHz, but not for remaining CF categories (Fig. 2*C*, pink bars vs. yellow bars; repeated-measures ANOVA; $P < 0.05$ for comparisons at CF categories of 1.5 and 3 kHz, but >0.05 for the rests).

Fig. 2*D* shows the distribution of CF values over the entire population of recording sites in each group. For NR rats, the percentage of A1 recording sites tuned to high frequencies was significantly larger than in CON rats, but was smaller for those tuned to low and middle frequencies (Fig. 2*D Left*; yellow bars vs. black bars; $\chi^2 = 27.8$; $P < 0.0001$). A similar tendency for CF distribution also was recorded in PNR rats (Fig. 2*D Left*; pink bars vs. black bars; $\chi^2 = 21.8$; $P < 0.0005$), manifesting changes in CF value distribution induced by noise exposure. For EXP rats, however, the percentage of A1 recording sites tuned to each frequency category was comparable to that seen in CON rats (Fig. 2*D Left*; blue bars vs. black bars; $\chi^2 = 1.17$; $P > 0.8$). These results are further
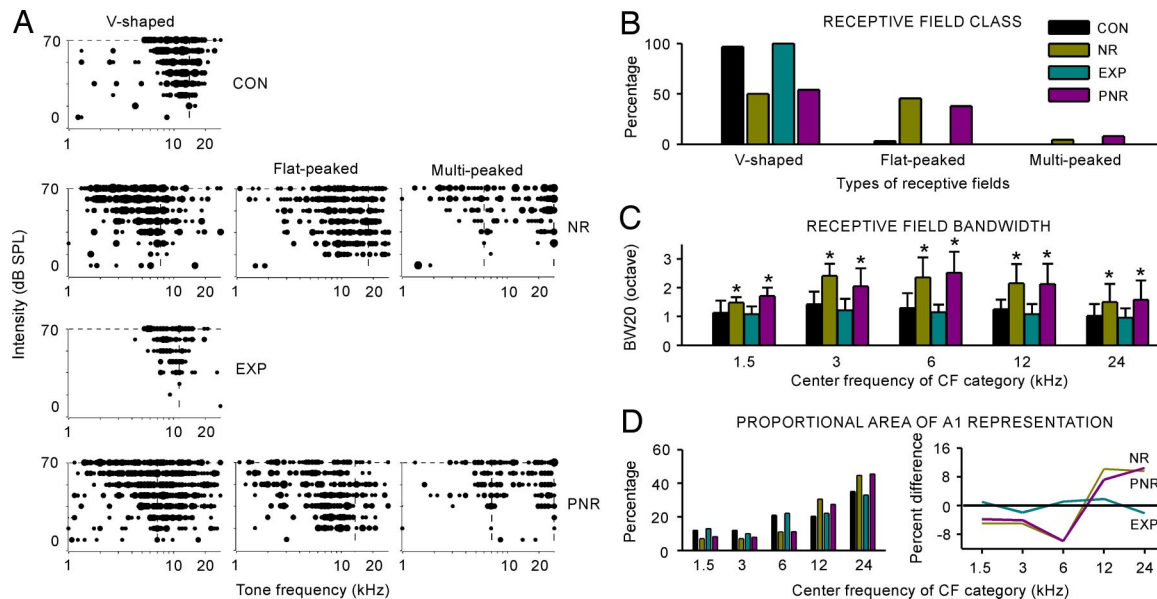
Fig. 2. Differences in neuronal response selectivity. (*A*) Representative examples of tonal receptive fields obtained from CON, NR, EXP, and PNR rats. Responses are represented by dots in the response area, with dot size proportional to the number of spikes evoked by tonal stimuli at each frequency and intensity. Dotted lines indicate positions of peaks of the receptive fields (marking CFs). (*B*) Distribution of receptive field types for all recordings obtained from four different rat groups. (*C*) Average receptive field BW20 for all recording sites in different groups of rats for each of five CF ranges. Values shown are mean ± SD. Bin size = 1 octave. *, $P < 0.001$. (*D*) Distribution of CF values for all recordings obtained from different groups of rats (*Left*) and difference functions calculated by subtracting the CF distribution in CON rats from that of NR, EXP, or PNR rats (*Right*). Zero values (solid black line) indicate no difference relative to the CF distribution of CON rats.

illustrated by plotting the same data as difference functions in Fig. 2*D Right*. Noise exposure in infancy decreased the area of representation for low frequencies and increased representational area of higher frequencies, compared with CON rats (Fig. 2*D Right*; yellow or pink line vs. black line). This representational distortion was normalized in EXP rats (Fig. 2*D Right*; blue line vs. black line).

A previous study has shown that perceptual learning induces substantial changes in the cortical encoding of sound intensity (19). Here we reexamined that effect by comparing the sound intensity thresholds obtained from different rat groups. As shown in Fig. 3*A*, thresholds of NR and PNR rats did not differ from those recorded in CON rats in any CF category (Fig. 3*A*, yellow or pink line vs. black line; repeated-measures ANOVA; $P > 0.05$ for both comparisons at each CF category). By contrast, thresholds recorded in EXP rats were significantly elevated when compared with those of CON rats in every CF category (Fig. 3*A*, blue line vs. black line; repeated-measures ANOVA; $P < 0.001$ for each comparison at different CF categories). This elevation ranged from an average of ≈12 dB for high-CF sites to ≈7 dB for low-CF sites. To further study the effect of training on intensity threshold, another group of NR rats ($n = 3$) was trained by using 50-dB sound pressure level (SPL) (i.e., 10

dB lower) target and nontarget sound stimuli. As expected, the average thresholds obtained from these rats were significantly lower than thresholds recorded in rats trained with 60-dB SPL (Fig. 3*B*, circle vs. triangle; repeated-measures ANOVA; $P < 0.05$ for comparison at each CF category). Although these thresholds also were consistently higher than those recorded in NR rats (by ≈2–4 dB) for every CF category, these differences were not significant (Fig. 3*B*, circle vs. yellow line; repeated-measures ANOVA; $P > 0.05$ for comparison at each CF category).

Finally, topographically ordered maps of A1 for sound frequency were obtained and compared for all groups. In CON rats, A1 was reliably identified by a continuous and complete low-to-high tonotopic gradient running caudal to rostral (Fig. 4*A Upper*). Large areas of A1 in NR and PNR rats, however, were occupied by neurons with poor frequency selectivity (i.e., neurons with flat- or multipeaked tuning curves marked as gray polygons in Fig. 4 *C Upper* and *D Upper*). After training, all sampled A1 sites in EXP rats had well defined CFs, and again tonotopic gradients in these animals were continuous and complete. Tonotopic organization in these EXP rats was undistinguished from that recorded in CON rats, but was sharply distinguished from that recorded in NR and PNR rats (Fig. 4 *B* vs. *A Upper*, *C Upper*, and *D Upper*).

To quantify the precision of the tonototicity within A1, the positions of each recording site in A1 were normalized with reference to the tonotopic axis and then plotted as a function of its CF. The average minimum distance from each site to the tonotopic axis was then calculated and used as an index of the precision (imprecision) in tonotopicity for each rat (see *Materials and Methods*). Each of these plots is shown below the tonotopic maps in Fig. 4. Sampling sites for CON and EXP rats were centered along the tonotopic axis, whereas those for NR and PNR rats were more widely scattered around the axis, resulting in an approximately two times larger index than CON and EXP rats (Fig. 4 *C* and *D* vs. *A Lower* and *B Lower*). Fig. 4*E* summarizes the average tonotopic indices obtained from different groups. Repeated-measures ANOVA showed that the indices of CON and EXP rats were
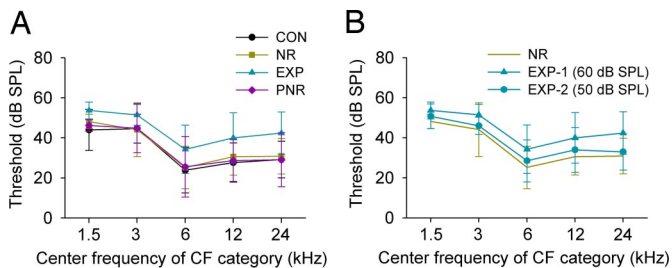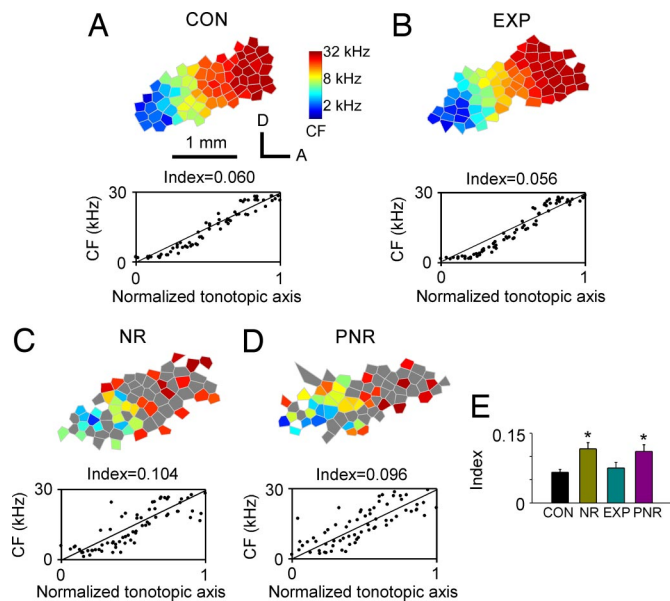

Fig. 3. Average intensity threshold at different CF ranges for CON ($n = 4$), NR ($n = 5$), EXP ($n = 5$), and PNR ($n = 5$) rats (*A*) and for EXP ($n = 3$) rats trained using 50-dB SPL sound stimuli (*B*). Values shown are mean ± SD.

Fig. 4. Topographic organization of A1. (*A–D*) (*Upper*) Representative maps illustrating the tonotopic organization within A1 recorded in CON, NR, EXP, and PNR rats. The color of each polygon indicates the CF (kHz) for neurons recorded at that site (see the scale to the right of *A Upper*). Polygons are Voronoi tessellations generated so that every point on the cortical surface was assumed to have the characteristics of its closest neighbors. Gray polygon in NR and PNR rats represents the flat- or multipeaked tuning curve recorded at that site. A, anterior; D, dorsal. (*A–D*) (*Lower*) Distribution of the cortical representation of different CFs along the tonotopic axis of the A1 for each example CF map. Normalized coordinates from each rat are plotted as a function of the defined CFs. Index (see *Materials and Methods*) of tonotopic orderliness is shown above each box. (*E*) Average tonotopic indices for CON, NR, EXP, and PNR rats. Values shown are mean ± SD. *, $P < 0.001$.

significantly smaller than those of NR and PNR rats ($P < 0.001$ for each comparison), manifesting more refined and differentiated tonotopic maps of CON and EXP rats than in NR and PNR rats.

To evaluate the long-term impact of perceptual training on cortical frequency representation, three additional EXP rats were returned to a neutral auditory environment after training cessation and then mapped at ≈P150 (i.e., 60 days after the end of perceptual training). The bandwidths of tuning curves and the tonotopic index were measured and compared with those of EXP rats mapped immediately after training cessation and with those of four age-matched CON rats. As summarized in Fig. 5, the data obtained from EXP rats mapped at ≈P150 were comparable to those obtained from EXP rats mapped immediately after training cessation. Both groups were substantially like those of CON rats (ANOVA; $P > 0.06$ for different comparisons), indicating a long-
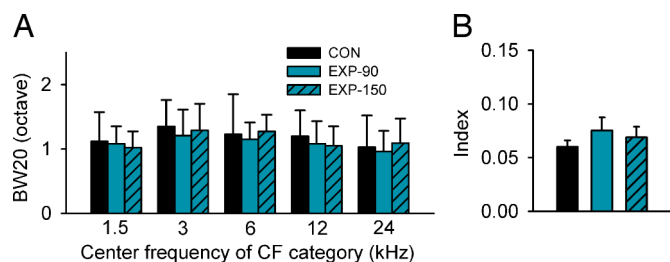
Fig. 5. Average BW20 (*A*) and tonotopic index (*B*) of EXP rats mapped immediately after training cessation (EXP-90) or ≈60 days after training cessation (EXP-150; $n = 3$) illustrated with age-matched CON rats ($n = 4$). Values shown are mean ± SD.

term conservation of training-induced changes on receptive field properties and tonotopicity in cortical field A1.

Discussion

In this study, NR rats were trained in an auditory frequency-recognition task by using a modified go/no-go training strategy, in which a target frequency was randomly set at the beginning of each day's training session. We found that the deteriorated cortical frequency representation induced by early postnatal (critical period) pulsed noise exposure was effectively normalized by this training, as shown by the observation that the number of V-shaped tuning curves, their sharpness as measured by BW20, and orderly tonotopicity as expressed by a tonotopic index were significantly increased when compared with those of NR controls. As a result, the cortical map and its constituent receptive fields in these representationally degraded-then-trained animals were equivalent to or even more refined than normal controls. This training-induced restoration of cortical frequency representations endured for at least 2 months after training cessation. No positive renormalization was recorded in control animals that were passively exposed to training stimuli. These results again show that perceptual learning strategies applied in postcritical-period animals can restore deteriorated auditory representations that stem from abnormal environments in early life.

Training-based auditory cortical plasticity has been previously reported in multiparametric sound domains (15–23). This plasticity is typically expressed as a change in receptive field bandwidths or preferential tuning, as well as selective modulation of firing rate to reinforced versus nonreinforced stimuli. An apparent virtue of the training strategy applied here was the extension of improvements in response selectivity and tonotopicity across a wide spectral range. By changing stimulus recognition targets daily and in random order, competitive cortical network changes presumably contributed to the differentiation of the selective representation of sound frequency inputs all across the frequency spectrum of hearing. This study thereby provides a useful model strategy for elaborating cortical representations in developmentally impaired human children. It should be noted that other studies have already shown that similar improvements can be generated for specific target stimuli in the spectral and intensive sound stimulus domains (20, 21) and for spectrotemporally complex acoustic inputs that distinguish speech phonemes (18, 43, 44). The use of roving targets (as is applied in training in this study) can almost certainly be used to sharpen cortical representations of all these sound parameters, contributing critically to complex signal (e.g., aural speech) representation. It might be noted that when animals were trained to discriminate tones of target frequencies from standard frequencies, both enhanced responses to target frequencies and reduced responses to nontarget frequencies were observed (16). The strategy applied here minimizes enduring negative plastic changes.

After closure of the critical period, tonotopic maps and response specificity of A1 neurons are not altered by unattended ambient auditory inputs (12, 13, 19, 45, 46). However, these studies once again demonstrate that the adult auditory cortex remains plastic for attended, rewarded stimuli. It has been suggested that the interaction of auditory inputs, neuromodulator release, and top–down influences from higher auditory areas contribute to this learning-based cortical plasticity (20, 47–55). The fact that passive exposure to the same stimuli, when not reliably coupled to reward, has no measurable effect on frequency selectivity and tonotopicity of A1 in the present study again supports the conclusion that top–down modulation contributes significantly to learning-induced cortical plasticity in the adult brain (20).

A final interesting finding of the current study was the alteration of A1 response thresholds altered by the intensive level of sound stimuli applied in the training. Previous studies have shown that learning-based cortical plasticity is restricted to the stimulus parameters that are relevant to the task demands (20, 21). For

example, animals trained to attend to frequency cues exhibit cortical reorganization only in the frequency domain, whereas animals trained to attend to intensity cues reorganize only in the intensity domain, although an identical set of auditory stimuli were used in both tasks (20). In the current study, all target (and nontarget) sounds were delivered at a constant sound intensity. If that intensity were relatively high (e.g., 60- to 70-dB SPL), the response thresholds of neurons with best frequencies spanning the spectral range of hearing in the rat were elevated so that these "best intensities" of neurons fell within this target range. If rats were trained at a lower sound intensity, the overall thresholds dropped presumably for the same reason. Thus, sound intensity also was a target-relevant domain, although the focus of training was sound frequency. Specialization of cortical processing to favor its operations over a given, narrower-than-normal intensive range is potentially limiting. This finding suggests that, for the most complete functional elaboration, stimuli should rove in frequency and intensity. This finding illustrates the importance of properly choosing sound parameters while applying learning-based training strategies.

In summary, previous studies demonstrate that perceptual training significantly modifies the representation and response selectivity of neurons in a normally developed adult A1. Here we extend those studies by showing that perceptual training also remediates the deteriorated frequency representation in adult A1 induced by early modulated noise exposure. A further study of the mechanisms underlying this training-based remediation of auditory representation should bear practical and theoretical importance, especially for those older children and adults suffering from hearing, language, and associated reading impairments.

Materials and Methods

All experimental procedures used in this study were approved by the Animal Care and Use Committees at the University of California, San Francisco.

Early Exposure of Rat Pups. Sprague–Dawley rat pups and their mothers were placed in a sound-shielded test chamber from P7 to P35. An 8-h light/16-h dark cycle was established. Fifty-millisecond noise pulses (5-msec ramps) delivered at 65-dB SPL were applied from a speaker placed ≈15 cm above the rats at five pulses per second at 1-sec intervals to minimize adaptation effects. Energy for noise stimuli was essentially flat across a broad frequency spectrum (0.2–30 kHz). No abnormalities in the behavior of either the mother or pups could be detected during pulsed noise exposure. The weights of all pups and mothers were continuously monitored, and there was no weight loss compared with naive rats, indicating normal lactation. Activity patterns during waking and sleep exhibited no evidence of stress.

After being reared from P7 to P35 in the presence of the pulsed noise in a sound chamber, rats were randomly divided into three groups: (*i*) NR rats, returned to a normal environment until A1 responses were documented; (*ii*) EXP rats, trained to identify a target auditory stimulus of specific frequency from a set of distractor stimuli (P36–P90); and (*iii*) PNR rats, passively exposed to training sounds that were identical to sounds delivered to EXP rats but given free access to food across the same epoch (P36–P90).

Behavioral Training. Rats assigned to the EXP group were trained to identify a target tonal stimulus with specific frequency (i.e., target frequency) amid a set of auditory stimuli of different frequencies. Stimuli were 60-dB SPL, 50-msec tone pips with 5-msec linear onset and offset ramps. Only one stimulus with specific frequency was presented in each trial. Rats were rewarded for making a go response within a limited time window after the target tone presentation. Training was conducted in an acoustically transparent operant training chamber (20 × 20 × 18 cm, length × width × height) enclosed within a sound-attenuated chamber. Stimuli were calibrated by using a Brüel & Kjær (Nærum, Denmark) micro-

phone and sound level meter, as well as a ubiquitous spectrum analyzer. Harmonics were of a low level and could not alter the representation of these recorded effects. An input and output system (photobeam detector, food dispenser, sound card, house light) was used to control behavioral training (Med Associates, Georgia, VT).

Rats were initially pretrained from P36 to P40 to make a nose poke only after presentation of a tonal stimulus at a fixed frequency of 6.5 kHz to obtain food reward. Starting from P41, tone stimuli with frequencies of 1.6, 2.1, 2.8, 3.7, 4.9, 6.5, 8.6, 11.4, 15.0, 19.9, or 26.2 kHz were randomly delivered during the training; one of these frequencies was randomly chosen as the target frequency at the beginning of each day's training session.

As in an earlier study from our laboratory (20), a single trial describes the length of time between the onset of two successive tones. The rats' behavior was reduced to go or no-go responses. Rats were in the go state when the photobeam was interrupted. All other states were considered no-go. For a given trial, rats could elicit one of five reinforcement states. The first four states were given by the combinations of responses (go or no-go) and stimulus properties (target or nontarget). Go responses within 3 sec of a target were scored as a hit; a failure to respond within this time window was scored as a miss. A go response within 3 sec of a nontarget stimulus was scored as a false positive, and the absence of a response was scored as a withhold. The fifth state, false alarm, was defined as a go response that occurred ≥3 sec after stimulus presentation. A hit triggered the delivery of a 45-mg food pellet (BioServe, Frenchtown, NJ). A miss, false positive, or false alarm initiated a 5-sec time-out period, during which the house lights were turned off and no stimuli were presented. A withhold did not produce a reward or a time out.

Trials were grouped into blocks of 100. Rats were trained for 1 block at the pretraining stage each day, but for 10 blocks at the full frequency stage. At the conclusion of each block, a target response ratio (number of hits/number of target trials) and a nontarget response ratio (number of false positives/number of nontarget trials) were calculated.

Electrophysiological Recording Procedure. Unless specified otherwise, electrophysiological recording of cortical responses was conducted at ≈P90 for all rats of different groups. In addition, A1 responses in age-matched naive female rats were documented as controls.

Rats were anesthetized with sodium pentobarbital (50 mg/kg body weight). Throughout the surgical procedures and during the recording session, a state of areflexia was maintained with supplemental doses of 8 mg/ml dilute pentobarbital injected i.p. The trachea was cannulated to ensure adequate ventilation, and the cisternae magnum was drained of cerebrospinal fluid to minimize cerebral edema. The skull was secured in a head holder, leaving the ears unobstructed. After reflecting the right temporalis muscle, the auditory cortex was exposed and the dura was resected. The cortex was maintained under a thin layer of viscous silicone oil to prevent desiccation.

Cortical responses were recorded with parylene-coated tungsten microelectrodes (1–2 MΩ at 1 kHz; FHC Inc., Bowdoinham, ME). Recording sites were chosen to evenly sample from the auditory cortex while avoiding blood vessels and were marked on a magnified digital image of the cortical surface vasculature. At each recording site, the microelectrode was lowered orthogonally into the cortex to a depth of 480–550 μm (layers 4 and 5), where vigorous stimulus-driven responses were recorded. Acoustic stimuli were generated by using TDT System III (Tucker-Davis Technologies, Inc., Alachua, FL) and delivered to the left ear through a calibrated earphone (STAX 54) with a sound tube positioned inside the external auditory meatus. A software package (SigCal, SigGen, and Brainware; Tucker-Davis Technologies, Inc.) was used to calibrate the earphone, generate acoustic stimuli, monitor cortical response

properties online, and store data for offline analysis. The evoked spikes of a neuron or a small cluster of neurons were collected at each site. Frequency-intensity receptive fields were reconstructed by presenting pure tones of 50 frequencies (1–30 kHz, 25-msec duration, 5-msec ramps) at eight sound intensities (0- to 70-dB SPL in 10-dB increments) to the contralateral ear in a random, interleaved sequence at a rate of two pulses per sec.

Cortical Mapping and Data Analysis. All analysis was performed offline with custom-written Matlab programs (The MathWorks, Natick, MA). The CF of a cortical site was defined as the frequency at the tip of the V-shaped tuning curve. For a flat-peaked tuning curve, CF was defined as the midpoint of the plateau at threshold. For tuning curve with multiple peaks, CF was defined as the frequency at the most sensitive tip (i.e., with lowest threshold). Response bandwidths (BW20s) were measured for all sites.

The area of A1 was defined as previously described (4). To generate A1 maps, Voronoi tessellation (a Matlab routine) was performed to create tessellated polygons, with the electrode penetration sites at their centers. Each polygon was assigned the characteristics (e.g., CF) of the corresponding penetration site. In this way, every point on the surface of the auditory cortex was linked to the characteristics experimentally derived from a sampled cortical site that was closest to this point.

We used an index to quantitatively describe the precision of tonotopicity in A1 (12, 13). The line connecting the two most anterior and posterior penetrations within A1 was used as a reference for tonotopic axis. We then rotated each map to orient the tonotopic axis horizontally. After rotation, new x coordinates of penetrations in each rat were normalized to be within a range from 0.0 to 1.0, and penetration sites were plotted according to their CFs and x coordinates. The logarithmic frequency range (1–30 kHz) was converted to a linear range (0–1). We defined the index as the average minimum distance from each data point to the line connecting (0, 0) and (1, 1). The larger the index, the more disordered the tonotopicity of the tonotopic map.

1. Chang EF, Merzenich MM (2003) *Science* 300:498–502.
2. Clements M, Kelly JB (1978) *Dev Psychobiol* 11:505–511.
3. Clopton BM, Winfield JA (1976) *J Neurophysiol* 39:1081–1089.
4. de Villers-Sidani E, Chang EF, Bao S, Merzenich MM (2007) *J Neurosci* 27:180–189.
5. Harrison RV, Stanton SG, Ibrahim D, Nagasawa A, Mount RJ (1993) *Acta Otolaryngol* 113:296–302.
6. Nakahara H, Zhang LI, Merzenich MM (2004) *Proc Natl Acad Sci USA* 101:7170–7174.
7. Poon PW, Chen X (1992) *Brain Res* 585:391–394.
8. Reale RA, Brugge JF, Chan JC (1987) *Brain Res* 431:281–290.
9. Sanes DH, Constantine-Paton M (1983) *Science* 221:1183–1185.
10. Sanes DH, Constantine-Paton M (1985) *J Neurosci* 5:1152–1166.
11. Stanton SG, Harrison RV (1996) *Audit Neurosci* 7:97–107.
12. Zhang LI, Bao S, Merzenich MM (2001) *Nat Neurosci* 4:1123–1130.
13. Zhang LI, Bao S, Merzenich MM (2002) *Proc Natl Acad Sci USA* 99:2309–2314.
14. Bao S, Chang EF, Woods J, Merzenich MM (2004) *Nat Neurosci* 7:974–981.
15. Beitel RE, Schreiner CE, Cheung SW, Wang X, Merzenich MM (2003) *Proc Natl Acad Sci USA* 100:11070–11075.
16. Blake DT, Strata F, Churchland AK, Merzenich MM (2002) *Proc Natl Acad Sci USA* 99:10114–10119.
17. Diamond DM, Weinberger NM (1986) *Brain Res* 372:357–360.
18. Fritz J, Shamma S, Elhilali M, Klein D (2003) *Nat Neurosci* 6:1216–1223.
19. Polley DB, Heiser MA, Blake DT, Schreiner CE, Merzenich MM (2004) *Proc Natl Acad Sci USA* 101:16351–16356.
20. Polley DB, Steinberg EE, Merzenich MM (2006) *J Neurosci* 26:4970–4982.
21. Recanzone GH, Schreiner CE, Merzenich MM (1993) *J Neurosci* 13:87–103.
22. Rutkowski RG, Weinberger NM (2005) *Proc Natl Acad Sci USA* 102:13664–13669.
23. Witte RS, Kipke DR (2005) *Brain Res Cogn Brain Res* 23:171–184.
24. Ahissar E, Vaadia E, Ahissar M, Bergman H, Arieli A, Abeles M (1992) *Science* 257:1412–1415.
25. Bao S, Chan VT, Merzenich MM (2001) *Nature* 412:79–83.
26. Edeline JM, Pham P, Weinberger NM (1993) *Behav Neurosci* 107:539–551.
27. Kilgard MP, Merzenich MM (1998) *Science* 279:1714–1718.
28. Merzenich MM (2001) In *Mechanisms in Cognitive Development*, eds McClelland J, Siegler R (Lawrence Erlbaum, Mahwah, NJ), pp 67–96.
29. Merzenich MM, Jenkins WM (1995) in *Maturational Windows and Adult Cortical Plasticity*, eds Julesz B, Kovacs I (Addison-Wesley, NY), pp 247–272.
30. Merzenich MM, Miller S, Jenkins W, Saunders G, Protopapas A, Peterson B, Tallal P (1998) in *Basic Neural Mechanisms in Cognition and Language*, ed Euler CV (Elsevier, Amsterdam), pp 143–172.
31. Merzenich MM, Saunders G, Tallal P (1999) in *Role of Neuroplasticity in Rare Developmental Disorders*, eds Broman S, Fletcher J (MIT Press, Cambridge, MA), pp 365–385.
32. Benasich AA, Tallal P (2002) *Behav Brain Res* 136:31–49.
33. Benasich AA, Choudhury N, Friedman JT, Realpe-Bonilla T, Chojnowska C, Gou Z (2006) *Neuropsychologia* 44:396–411.
34. Choudhury N, Benasich AA (2003) *J Speech Lang Hear Res* 46:261–272.
35. Ahissar M, Protopapas A, Reid M, Merzenich MM (2000) *Proc Natl Acad Sci USA* 97:6832–6837.
36. Bailey PJ, Snowling MJ (2002) *Br Med Bull* 63:135–146.
37. Banai K, Ahissar M (2006) *Cereb Cortex* 16:1718–1728.
38. Tallal P (2004) *Nat Rev Neurosci* 5:721–728.
39. Tallal P, Piercy M (1973) *Nature* 241:468–469.
40. Merzenich MM, Jenkins WM, Johnston P, Schreiner C, Miller SL, Tallal P (1996) *Science* 271:77–81.
41. Tallal P, Miller SL, Bedi G, Byma G, Wang X, Nagarajan SS, Schreiner C, Jenkins WM, Merzenich MM (1996) *Science* 271:81–84.
42. Tallal P, Merzenich MM, Miller S, Jenkins W (1998) *Scand J Psychol* 39:197–199.
43. Fritz J, Elhilali M, Shamma S (2005) *J Neurosci* 25:7623–7635.
44. Fritz J, Elhilali M, Shamma S (2005) *Hear Res* 206:159–176.
45. Ohl FW, Scheich H (2005) *Curr Opin Neurobiol* 15:470–477.
46. Weinberger NM (1995) *Annu Rev Neurosci* 18:129–158.
47. Bao S, Chan VT, Merzenich MM (2001) *Nature* 412:79–83.
48. Bao S, Chan VT, Zhang LI, Merzenich MM (2003) *Proc Natl Acad Sci USA* 100:1405–1408.
49. Bakin JS, Weinberger NM (1990) *Brain Res* 536:271–286.
50. Bakin JS, Weinberger NM (1996) *Proc Natl Acad Sci USA* 93:11219–11224.
51. Ji W, Gao E, Suga N (2001) *J Neurophysiol* 86:211–225.
52. Kilgard MP, Merzenich MM (1998) *Nat Neurosci* 1:727–731.
53. Kilgard MP, Pandya PK, Vazquez J, Gehi A, Schreiner CE, Merzenich MM (2001) *J Neurophysiol* 86:326–338.
54. Kilgard MP, Pandya PK, Engineer ND, Moucha R (2002) *Biol Cybern* 87:333–343.
55. Weinberger NM (2004) *Nat Rev Neurosci* 5:279–290.